Stochastic model refinements for GOCE gradiometry data

Krasbutter I., Brockmann J.M., Kargoll B., Schuh W.-D.

Institute of Geodesy and Geoinformation, Department of Theoretical Geodesy, University of Bonn, Nussallee 17, 53115 Bonn, Germany, E-Mail: krasbutter@geod.uni-bonn.de

Abstract

In our approach to gravity field determination, the GOCE data are processed sequentially on a parallel computer system, iteratively via application of the method of preconditioned conjugate gradient multiple adjustment (PCGMA), and in situ via development of the functionals at the actual location and orientation of the gradiometer. GOCE gradiometry (SGG) data are auto-correlated in their three components Vxx, Vyy and Vzz so that one purpose of PCGMA is the adjustment of the unknown stochastic model of the gradiometer observations, described by decorrelation filters. A sequence of AutoRegressive-Moving Average (ARMA) filters is adjusted to the actual measurement noise to remove these correlations from the observations. This adjustment is refined iteratively, as it is embedded in the estimation of the gravity field parameters. In this contribution we show the effects of various filter complexities on the final gravity field solution and the corresponding error estimates based on two months of GOCE data.

1. Introduction

The Tuning Machine, as part of ESA's High-Level Processing Facility (HPF), was designed with the purpose of tuning the stochastic model of the gravity gradients observed by GOCE's gradiometer and to obtain an independent gravity field solution (cf. *Pail et al. 2006, Brockmann et al. 2010, Schuh et al. 2010*). Based on this gravity field model, the final solution of the so-called time-wise approach (cf. *Pail et al. 2006, Pail et al. 2010)* is computed at TU Graz. The gravity field solution is determined by applying an iterative solver based on the method of preconditioned conjugate gradients (cf. *Schuh 1996, Boxhammer 2006*) and the corresponding covariance matrix by means of Monte-Carlo methods (cf. *Alkhatib 2007*).

In this paper we will demonstrate how the information content of the gravity gradient noise is effectively taken into account with the time-wise approach. In Sect. 2 we show the general characteristics of the real-data noise, and in Sect. 3 the effects of various approaches to modeling these characteristics by means of digital filters on the gravity field solution and its accuracies.

2. Characteristics of the gradiometer noise

To obtain a first impression of the gradiometer noise characteristics we determined the difference between mean- and GRS80-reduced measured gravity gradients (light gray curve) and mean- and GRS80-reduced gravity gradients computed from an a priori gravity field model (dark gray curve), see Fig. 1 This difference (black curve) serves as a first estimation of the unknown gradiometer noise (the three diagonal components Vxx, Vyy and Vzz show a very similar behavior, which is why only the Vzz component is depicted here). This noise estimate is seen to be of similar magnitude as the measured gravity field signal and to have low-frequency oscillations, indicating strong autocorrelatedness.

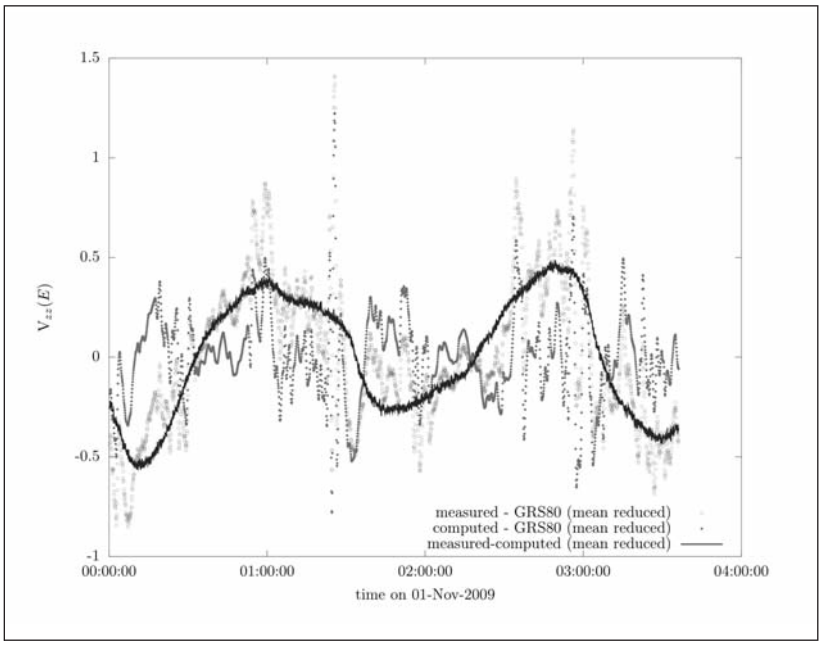

Figure 1: Reduced (mean and GRS80) measured gravity field gradients of GOCE for 3 hours and computed gravity field gradients from a gravity field model and the difference as a first estimation for the gradiometer

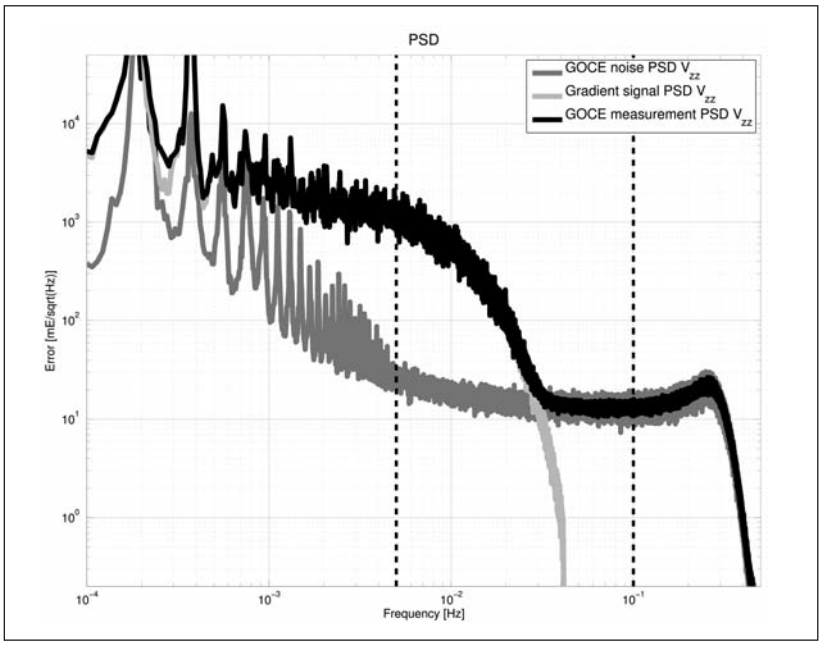

Figure 2: Power spectrum (PSD) of the gradiometer noise for the Vzz component, the gradient signal and the measured gravity gradients

These significant autocorrelations indicate that the noise is generated by a colored noise process, the details of which become more clearly visible after transforming the autocorrelation function of the noise time series into the spectral domain (see dark gray curve in Fig. 2).
Within the measurement bandwidth (MBW, between 0.005 and 0.1 Hz), the power spectrum (PSD) is practically flat, i.e. white; between 0 and 0.005 Hz the spectrum is mainly characterized by an inverse proportional dependence (approx. 1/f) and a large number of sharp peaks. This reflects exactly the expected behavior, which was revealed by various case studies carried out before the satellite's launch (e.g. *Schuh et al. 2006*).

As the gravity field parameters are determined via a rigorous least-squares adjustment, this autocorrelation pattern must be taken into account by including the known (or an estimated approximation of the) data covariance matrix. However, due to the huge number of gradiometer data, this covariance matrix can-

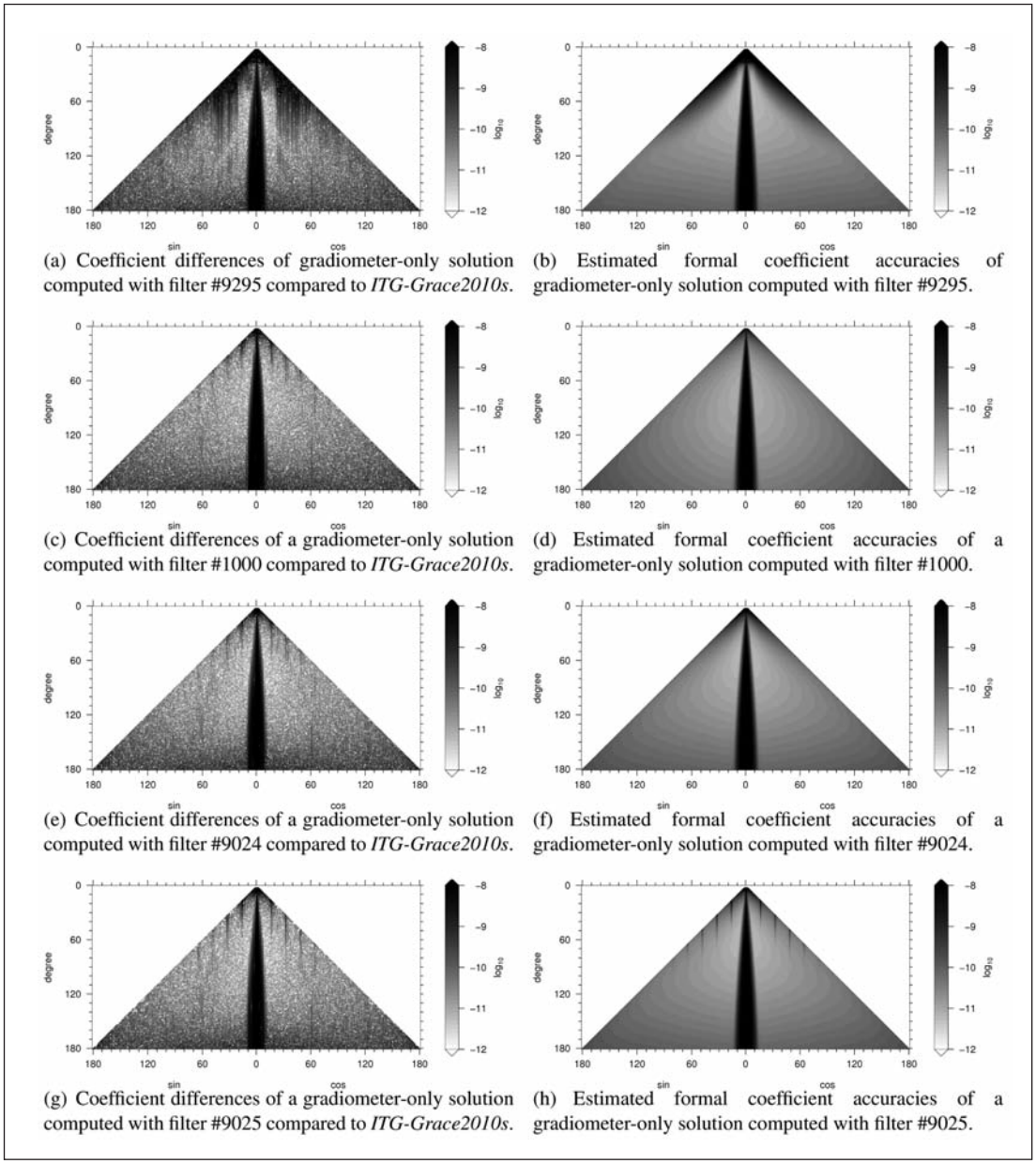

(a) Coefficient differences of gradiometer-only solution computed with filter #9295 compared to *ITG-Grace2010s*.

(b) Estimated formal coefficient accuracies of gradiometer-only solution computed with filter #9295.

(c) Coefficient differences of a gradiometer-only solution computed with filter #1000 compared to *ITG-Grace2010s*.

(d) Estimated formal coefficient accuracies of a gradiometer-only solution computed with filter #1000.

(e) Coefficient differences of a gradiometer-only solution computed with filter #9024 compared to *ITG-Grace2010s*.

(f) Estimated formal coefficient accuracies of a gradiometer-only solution computed with filter #9024.

(g) Coefficient differences of a gradiometer-only solution computed with filter #9025 compared to *ITG-Grace2010s*.

(h) Estimated formal coefficient accuracies of a gradiometer-only solution computed with filter #9025.

Figure 3: Coefficient statistics for all four presented gradiometer solutions with the four different filters. The shown statistics are: differences to the ITG-Grace2010s model (left column) and estimated formal coefficient standard deviations (right column)

not be stored in light of memory requirements of more than 20 PetaByte. An effective solution to this problem consists in a full decorrelation (»whitening«) of the gradiometer data before the adjustment is carried out. In the next section we show how such a decorrelation is performed through an application of digital filters (cf. *Schuh 1996, Siemes 2008 and Krasbutter 2009*).

3. Modeling the gradiometer noise

The colored noise characteristics of the gradiometer is taken into account by filtering the observations with a filter that has the inverse spectral characteristics with regard to the estimated noise charateristics as seen in the previous section. Such a filter acts as a decorrelation filter and can be modeled by means of cascades of ARMA processes (*Schuh 1995, Schuh 1996 and Siemes 2008*). As ARMA filters can be designed with an increasing num-

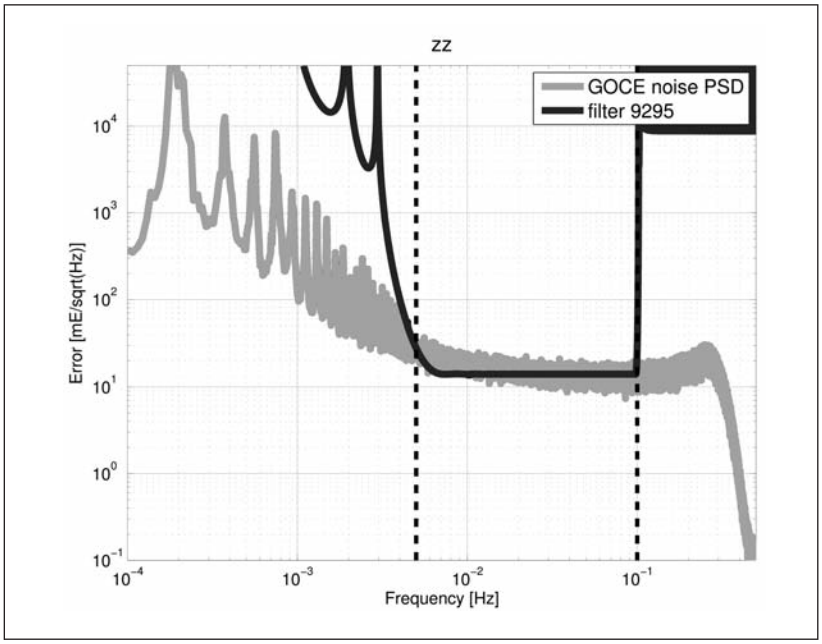

Figure 4: Noise power spectrum and inverse power spectrum of decorrelation filter # 9295 (MBW band-pass filter) w.r.t. the Vzz component (the other components show a similar behavior)

ber of free parameters to fit more and more details of the power spectrum the question arises how much the gravity field solution gains in accuracy when very detailed (and thus computationally more demanding as well as numerically more instable) ARMA filters are used in comparison to simpler filters. This question is investigated by fitting four types of ARMA filters to specific features of the spectrum.

3.1. Modeling of the MBW only

In the case that only the MBW is taken into account within the decorrelation process, a band-pass filter can be used (cf. Fig. 4), which cuts out the entire information outside the MBW. Gravity field determination with such a kind of filter is possible, but has certain disadvantages, as demonstrated in the following. A gradiometer-only gravity field solution computed with this filter is shown in terms of coefficient differences with respect to a GRACE-only model based on seven years of data and resolved up to degree and order (d/o) 180 ITG-Grace2010s, cf. *Mayer-Gürr et al. (2010)*.

Fig. 3 (a) shows that these differences are very large up to d/o 50 (the GRACE model is considered as a reference solution up to d/o 140, as GRACE is more sensitive to the lower degrees than GOCE gradiometry). In addition, large differences occur for the sectorial coefficients from d/o 50 up to d/o 100. This behavior of the sectorial and near-sectorial coefficients is reflected by the estimated spherical harmonic coefficient accuracies shown in Fig. 3 (b). For d/o 80 up to 140, the differences to the GRACE model can be explained by the corresponding GOCE accuracies.

Thus, using a band-pass filter as shown in Fig. 4 produces a useful gradiometer-only gravity field and realistic estimates for the coefficient variances, but has the disadvantage that gradiometer information in the lower frequencies is ignored which affects the sectorial coefficients up to d/o 100.

3.2 Modeling the low-frequency part of the spectrum

As the band-pass filter of Sect. 3.1 was seen to produce systematic errors for the sectorial coefficients, it is advisable to also model the low-frequency noise characteristics. Such a filter should not completely filter out the low-frequency part of the power spectrum, but reflect its low accuracy when applied as a decorrelation filter in gravity field determination. The simplest filter of this kind is a differencing filter (#1000) as shown in Fig. 5.

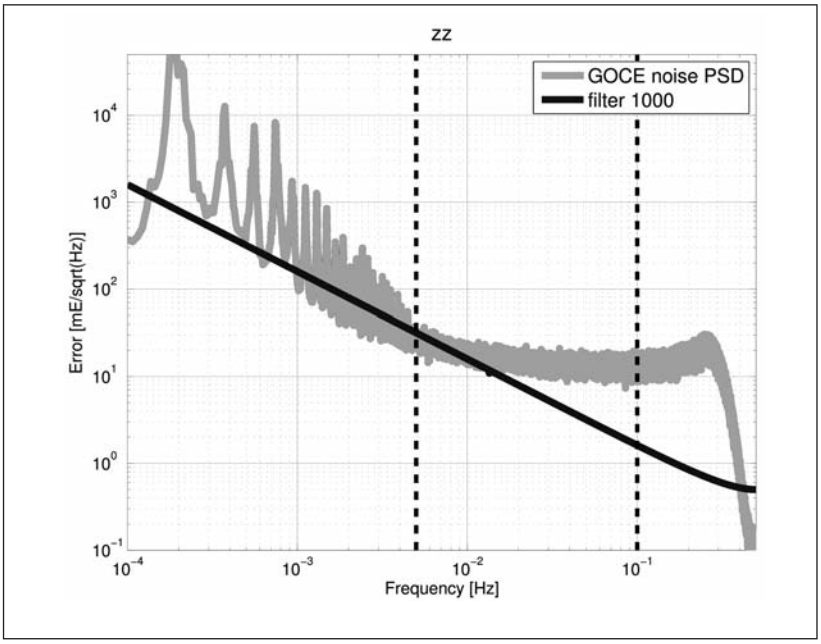

Figure 5: Noise power spectrum and inverse power spectrum of decorrelation filter # 1000 (differencing filter) w.r.t. the Vzz component (the other components show a similar behavior)

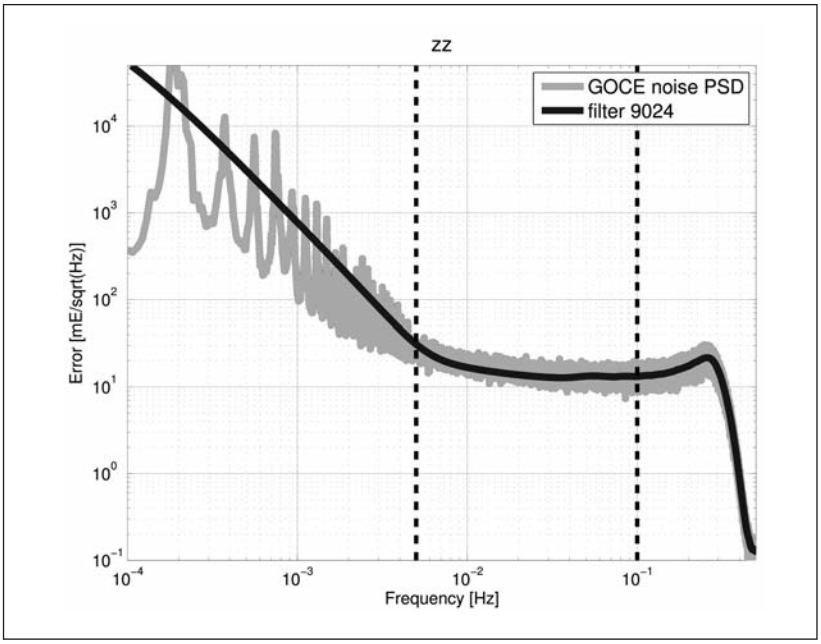

Figure 6: Noise power spectrum and inverse power spectrum of decorrelation filter # 9024 w.r.t. the Vzz component (the other components show a similar behavior)

A comparison of a gradiometer-only gravity field solution using this filter with a GRACE model is shown in Fig. 3 (c). It can be seen that the lower degree differences (up to d/o 80) are smaller than the corresponding degree differences based on the solution with a band-pass decorrelation filter (determined in Sect. 3.1). In addition, Fig. 3 (d) shows that the sectorial coefficients of d/o 20 and higher are determined more precisely in this case (compared to Fig. 3(b)) which is a desirable consequence of having taken into account the low-frequency part of the power spectrum. However, as the differencing filter does not reflect the MBW as accurately as the band-pass filter, the variances of the higher degrees and orders cannot be estimated as realistically. To avoid the undesirable features of the band-pass and the differencing filter, both filter characteristics can be combined as demonstrated in the following.

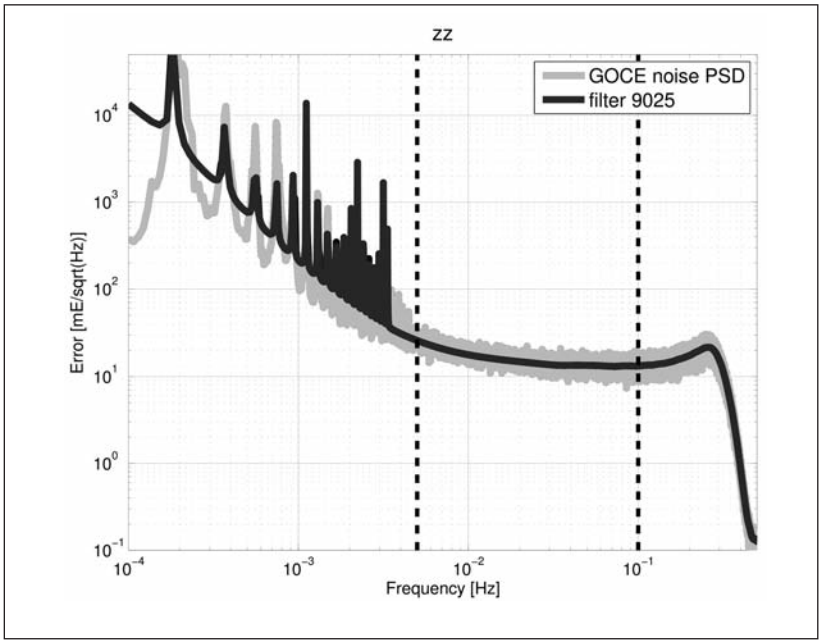

Figure 7: Noise power spectrum and inverse power spectrum of decorrelation filter # 9025 w.r.t. the Vzz component (the other components show a similar behavior)

3.3. Simple modeling of the complete spectrum

Combining the features of a band-pass and a differencing filter yields a simple filter model for the entire spectrum. Such a filter is represented by a sequence (cascade) of basic ARMA filters. Fig. 6 (filter # 9024) shows the spectral characteristics of a parsimonious cascade of ARMA filters, which nevertheless represents an apparently overall adequate fit to the noise characteristics, but ignores the sharp peaks in the low-frequency part of the spectrum.

The resulting gravity field solution (see Fig. 3 (e) and 3 (f)) combines the advantages of the band-pass filter solution and the difference filter solution: both the low-degree and the sectorial coefficients are determined accurately and the variances for the higher d/o coefficients are estimated more realistically than for the filter models used in Sect. 3.1 and 3.2.

3.4. Detailed modeling of the complete spectrum

Extending the ARMA filter cascade of the pervious Sect. 3.3 to also take into account the sharp spectral peaks leads to a more complex decorrelation filter as shown in Fig. 7. These peaks are modeled by means of notch filters, represented by 20 additional individual ARMA(2,2) filters.

Although such detailed modeling of the complete spectrum does not lead to a significant improvement of the solution (see Fig. 3 (g)), it evidently leads to far more realistic accuracy estimates (see Fig. 3 (h)). The error pattern with stripes occuring for degrees 16, 32,..., which is already clearly visible in the coefficient differences with respect to the ITG-Grace2010s solution (cf. Fig. 3 (g)), is now correctly mapped into the coefficients' covariance matrix (cf. Fig. 3 (h)).

4. Summary and conclusions

Much effort has been put into the refinement of the stochastic model of GOCE gradient measurements and matching digital decorrelation filters to obtain not only a realistic gravity field solution but also a corresponding realistic full covariance matrix. It must be stressed that the estimated spherical harmonic coefficients must be consistent with the corresponding accuracy estimates in order to provide meaningful GOCE-only gravity field information that can be used in a multitude of applications e.g. in geodesy, geophysics, and oceanography. Filter # 9024, which represents a simple decorrelation filter model for the entire gradiometer noise power spectrum (as described in Sect. 3.3), was applied for the computation of the

global gravity field model GO_CONS_GCF_2_TIM, which is based on the time-wise approach and constitutes one of the first GOCE-only gravity field models (*Pail et al 2010*).

Acknowledgments

This work was financially supported by the BMBF Geotechnologien program REAL-GOCE. GOCE data access was granted by ESA GOCE HPF main contract No. 18308/04/NL/MM. The computations were performed on the JUROPA supercomputer in Jülich. The computing time was granted by John von Neumann Institute for Computing (project HBN15).

References

Alkhatib, H. (2007) On Monte Carlo methods with applications to the current satellite gravity missions. Dissertation, http://hss.ulb.uni-bonn.de/2007/1078/1078.htm, Institute of Geodesy and Geoinformation, University of Bonn.

Boxhammer, C. (2006) Effiziente numerische Verfahren zur sphärischen harmonischen Analyse von Satellitendaten. Dissertation, Institute of Geodesy and Geoinformation, http://hss.ulb.uni-bonn.de/2006/0799/0799.htm, University of Bonn.

Brockmann, J.M., B. Kargoll, I. Krasbutter, W.-D. Schuh and M. Wermuth (2010) GOCE Data Analysis: From Calibrated Measurements to the Global Earth Gravity Field. Flechtner, F., T. Gruber, A. Güntner, M. Mandea, M. Rothacher, T. Schöne and J. Wickert (eds.), System Earth via Geodetic-Geophysical Space Techniques, Advanced Technologies in Earth Sciences, Springer Berlin Heidelberg, 213-229.

Krasbutter, I. (2009) Dekorrelation und Daten-TÜV der GOCE-Residuen. Diploma thesis, Universität Bonn.

Mayer-Gürr, T, E. Kurtenbach and A. Eicker (2010), ITG-GRACE2010. http://www.igg.unibonn.de/apmg/ index.php?id=itg-grace2010, 2010.

Pail, R., B. Metzler, B. Lackner, T. Preimesberger, E. Höck, W.-D. Schuh, H. Alkathib, C. Boxhammer, C. Siemes and M. Wermuth (2006) GOCE gravity field analysis in the framework of HPF: operational software system and simulation results. In: 3. GOCE user workshop. ESA, Frascati.

Pail, R., H. Goiginger, R. Mayrhofer W.-D. Schuh, J.M. Brockmann, I. Krasbutter, E. Höck and T. Fecher (2010) Global gravity field model derived from orbit and gradiometry data applying the time-wise method. In: ESA Living Planet Symposium, ESA Living Planet Symposium. SP-686, Bergen.

Schuh, W.-D. (1996) Tailored Numerical Solution Strategies for the Global Determination of the Earth's Gravity Field, Vol. 81 Mitteilungen der geodätischen Institute der Technischen Universität Graz. TU Graz.

Schuh, W.-D., C. Boxhammer and C. Siemes (2006) Correlations, variances, covariances - from GOCE signals to GOCE products. In: 3. GOCE user workshop. ESA, Frascati.

Schuh, W.-D., J.M. Brockmann, B. Kargoll and I. Krasbutter (2010) Adaptive Optimization of GOCE Gravity Field Modeling. In: Münster, G., D. Wolf and M. Kremer (eds.), NIC Symposium 2010, Vol. 3 IAS Series. Jülich, Germany, 313-320.

Schuh, W.D. (1995) SST/SGG tailored numerical solution strategies. ESA-Project CIGAR III / Phase 2, WP 221, Final-Report, Part 2.

Siemes, C. (2008) Digital Filtering Algorithms for Decorrelation within Large Least Squares Problems. Dissertation, http://hss.ulb.uni-bonn.de/2008/1374/1374.htm, Institute of Geodesy and Geoinformation, University of Bonn.